IEEE Access
Multidisciplinary | Rapid Review | Open Access Journal

Received December 3, 2018, accepted December 18, 2018, date of publication December 24, 2018, date of current version February 8, 2019.

Digital Object Identifier 10.1109/ACCESS.2018.2889504

Observer-Based Leader-Following Formation Control for Multi-Robot With Obstacle Avoidance

XIRU WU[1,2], SHANSHAN WANG[1], AND MENGYUAN XING[1]

[1]College of Electronic Engineering and Automation, Guilin University of Electronic Technology, Guilin 541004, China
[2]Guangxi Key Laboratory for Nonlinear Circuit and Optical Communication, Guangxi Normal University, Guilin 541004, China

Corresponding author: Xiru Wu (xiruwu@guet.edu.cn)

This work was supported in part by the National Natural Science Foundation of China under Grant 61603107, Grant 61863007, and Grant 61863008, in part by the Guangxi Key Laboratory for Nonlinear Circuit and Optical Communication (Guangxi Normal University) under Grant NCOC2016-B01, in part by the Innovation Project of Guangxi Graduate Education under Grant YCSW2017144, in part by the Innovation Project of GUET Graduate Education under Grant 2017YJCX88 and Grant 2018YJCX76, and in part by the Excellent Dissertation Training Program of GUET Graduate Education under Grant YXYJBX39.

ABSTRACT This paper focuses on the observer-based leader-following formation tracking control for multi-robot with obstacle avoidance. First, based on the leader-follower formation control method, setting the trajectory of the leader robot, then the follower robots track the leader robot. Second, an observer for the followers is designed to estimate the state of the leader robot, which can limit the estimation errors to a small value at short time-frame. Moreover, the gain controller and corrective controller are presented to complete the formation task and implement the trajectory transformation, respectively. In addition, an improved obstacle avoidance algorithm is devised to avoid the obstacles by adjusting the angle between the leader robot and the followers. Finally, the simulation results are presented to verify the effectiveness of the proposed control scheme. The main advantages of this paper are both an observer-based controller includes gain control and corrective control is developed for the nonlinear multi-robot system, and the obstacle avoidance problem during movement is solved with the optimal method.

INDEX TERMS Multi-robot, formation control, observer-based, obstacle avoidance.

I. INTRODUCTION

Recently, control problems of robot have gained a lot of attention and developed rapidly owing to their extensive applied space. A number of great theoretical significance results have been reported in the literature [1]–[5]. Formation control, an important part in the cooperative area of multi-robot have always been the hottest research topics. There are many approaches have been applied for both theoretical research and engineering applications, such as behavior-based [6], potential field-based [7], [8], leader-follower [9]–[11], graph theory-based [12] and virtual structure [13], etc. To guarantee the consensus of position and direction for the multiple robots, a backstepping-based controller was put forward by Cao *et al.* [14]. In [15], to figure out the indeterminate relative distance, robust adaptive controller was presented using the dynamic estimation of the distance between leader and followers. Xing *et al.* [16] designed the distributed nonlinear controller with fixed-time properties for the multi-robot system to solve the formation tracking problem. In [17], a formation control approach was designed according to the distance and orientation for any arbitrary undirected communication graph.

In the past few years, observer has been widely applied to the formation control [18]–[21]. For example, augmented fuzzy observer was put forward in [22] to implement synchronous estimation of the system state and the disturbance term. In [23], the integral action was incorporated into the observer controller to improve the formation tracking and observation performance. To guarantee the consensus of general linear multi-robot systems, observer-based event-triggered approach was presented by Wang *et al.* [24]. Wen *et al.* [25] developed the distributed controller based on a reduced-order state observer to track the high-dimensional leader robot. An adaptive observer-based sliding mode controller was applied in [26] to estimate the velocity from the position of noisy. In the existing results, there are few literatures to consider the sudden change of the given trajectory.

At present, obstacle avoidance is a key problem to be addressed urgently in multi-robot system. In practice, the robots must avoid colliding with other robots as well as with obstacles [27], [28]. For instance, in [29], Panagou and Kumar proposed the feedback control strategy that the leader completes obstacle avoidance whereas the followers ensure visibility maintenance of robots. In [30], particle swarm optimization was introduced to achieve the formation control without a significant increase for computational complexity. The artificial potential field approach and leader-follower formation method were combined together to complete obstacle avoidance by Wen *et al.* [31]. Mylvaganam and Sassano [32] designed the collision-free trajectories to satisfy the single-integrator dynamics by exploiting a differential game formulation. Comparing with obstacle avoidance algorithm in the literatures [29]–[32], in this paper, not only the obstacle avoidance between the robots and the obstacles is discussed, but also the collision avoidance between robots is considered.

Motivated by the above analysis, in this paper, the position tracking and the obstacle avoidance for the multi-robot system are discussed. The main contributions of the research described are threefold. First, an observer is devised to estimate the state of the leader robot. Second, the formation controller which includes gain control and corrective control is presented to complete the formation task and implement the trajectory transformation. Finally, IOAA is proposed to avoid obstacle by adjusting the angle between the leader robot and the follower robots, which can decrease the allocation of time.

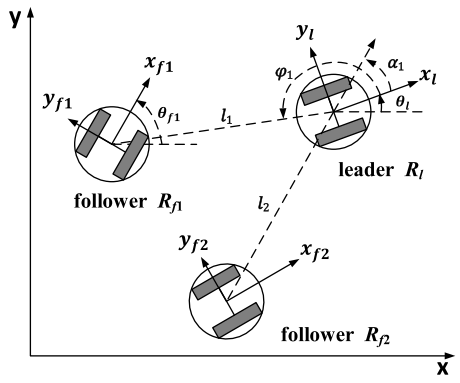

FIGURE 1. Leader-follower formation model.

II. LEADER-FOLLOWING FORMATION CONTROL

A. LEADER-FOLLOWER KINEMATIC MODEL

The leader-follower formation model is shown in Fig. 1. The discrete-time mathematical model of the robot R can be abstracted as:

$$\begin{cases} x_{k+1} = x_k + T_c v_k \cos\theta_k \\ y_{k+1} = y_k + T_c v_k \sin\theta_k \\ \theta_{k+1} = \theta_k + T_c \omega_k, \end{cases} \tag{1}$$

where (x, y) denotes the position, θ is the orientation, v and ω express the linear velocity and angular velocity, T_c represents the sampling period.

In this paper, the unicycle's center is associated with the world's reference frame. In Fig. 1, φ_i represents the view angle from the x-axis of the leader robot to the centroid of the follower robot, l means the distance between the center of the leader and the followers, and α_n is the relative orientation of the leader robot and the follower robots, i.e., $\alpha_n \triangleq \theta_{fn} - \theta_l$, $n = 1, 2, 3, \cdots, n$.

B. THE NONLINEAR STATE ESTIMATOR

To design the controller for the leader-follower formation, the nonlinear multi-robot system can be written as

$$\Sigma : \begin{cases} \boldsymbol{s}_{k+1} = f_k(\boldsymbol{s}_k, \boldsymbol{u}_k) \\ \boldsymbol{Q}_{k+1} = h_{k+1}(\boldsymbol{s}_{k+1}), \end{cases} \quad s.t.\ \boldsymbol{P}(\boldsymbol{s}_{k+1}) = \boldsymbol{p}_{k+1}, \tag{2}$$

where $\boldsymbol{s}_k = \begin{bmatrix} x_k & y_k & \theta_k \end{bmatrix}^T$ expresses the state vector, $\boldsymbol{u}_k = \begin{bmatrix} v_k & \omega_k \end{bmatrix}^T$ is the control vector, $\boldsymbol{Q}_{k+1}$ denotes the output vector; $\boldsymbol{P}(\boldsymbol{s}_{k+1})$ shows linear or nonlinear function, and $\boldsymbol{p}_{k+1}$ represents the desired tracking trajectory.

The predict estimation of the state vector $\hat{\boldsymbol{s}}_{k+1|k}$ and the output vector $\hat{\boldsymbol{Q}}_{k+1|k}$ can be shown as

$$\Sigma : \begin{cases} \hat{\boldsymbol{s}}_{k+1|k} = f_k\left(\hat{\boldsymbol{s}}_{k|k}, \boldsymbol{u}_k\right) \\ \hat{\boldsymbol{Q}}_{k+1|k} = h_{k+1}\left(\hat{\boldsymbol{s}}_{k+1|k}\right). \end{cases} \tag{3}$$

The filter estimation of the state vector $\hat{\boldsymbol{s}}_{k+1|k+1}$ and the output vector $\hat{\boldsymbol{Q}}_{k+1|k+1}$ are given by

$$\Sigma : \begin{cases} \hat{\boldsymbol{s}}_{k+1|k+1} = \hat{\boldsymbol{s}}_{k+1|k} + \boldsymbol{L}_{k+1}\left(\boldsymbol{Q}_{k+1} - \hat{\boldsymbol{Q}}_{k+1|k}\right) \\ \hat{\boldsymbol{Q}}_{k+1|k+1} = h_{k+1}\left(\hat{\boldsymbol{s}}_{k+1|k+1}\right), \end{cases} \tag{4}$$

where $\boldsymbol{L}_{k+1}$ shows the observer gain.

Assuming that the true state $\boldsymbol{s}_k$ is close to the estimate state $\hat{\boldsymbol{s}}_{k|k}$. Expressing $f_k(\boldsymbol{s}_k, \boldsymbol{u}_k)$ with the first order approximation as follows

$$f_k(\boldsymbol{s}_k, \boldsymbol{u}_k) = f_k\left(\hat{\boldsymbol{s}}_{k|k}, \boldsymbol{u}_k\right) + \hat{\boldsymbol{A}}_k\left(\boldsymbol{s}_k - \hat{\boldsymbol{s}}_{k|k}\right), \tag{5}$$

where $\hat{\boldsymbol{A}}_k = \frac{\partial f_k(\hat{\boldsymbol{s}}_{k|k}, \boldsymbol{u}_k)}{\partial \boldsymbol{s}_k}$.

Similarly, $h_{k+1}(\boldsymbol{s}_{k+1})$ can be written as

$$h_{k+1}(\boldsymbol{s}_{k+1}) = h_{k+1}\left(\hat{\boldsymbol{s}}_{k+1|k}\right) + \hat{\boldsymbol{C}}_{k+1}\left(\boldsymbol{s}_{k+1} - \hat{\boldsymbol{s}}_{k+1|k}\right), \tag{6}$$

where $\hat{\boldsymbol{C}}_{k+1} = \frac{\partial h_{k+1}(\hat{\boldsymbol{s}}_{k+1|k})}{\partial \boldsymbol{s}_{k+1}}$.

Defining the filter estimation error as $\boldsymbol{e}_{s_{k+1|k+1}}$ and combining (2)-(6), we get

$$\boldsymbol{e}_{s_{k+1|k+1}} = \boldsymbol{s}_{k+1} - \hat{\boldsymbol{s}}_{k+1|k+1} = \boldsymbol{A'}_k\left(\boldsymbol{s}_k - \hat{\boldsymbol{s}}_{k|k}\right), \tag{7}$$

where $\boldsymbol{A'}_k = \left(\boldsymbol{I} - \boldsymbol{L}_{k+1}\hat{\boldsymbol{C}}_{k+1}\right)\hat{\boldsymbol{A}}_k$.

C. OBSERVER-BASED CONTROLLER

The control strategy is divided into two components, the gain control and the corrective control. The formation tracking controller can be designed to

$$\boldsymbol{u}_k = \boldsymbol{u'}_{k-1} + \boldsymbol{u''}_k + \Delta\boldsymbol{u'}_{k-1} + \Delta\boldsymbol{u''}_k \tag{8}$$

where $\boldsymbol{u'}_{k-1}$ and $\boldsymbol{u''}_k$ are the gain and the corrective components at the $(k-1)^{th}$ sample time respectively. $\Delta\boldsymbol{u'}_{k-1}$ and $\Delta\boldsymbol{u''}_k$ denote the incremental change in the gain part and the corrective component respectively.

1) GAIN CONTROL

The gain control signal $\Delta\boldsymbol{u'}_{k-1}$ is designed. $\Delta\boldsymbol{u''}_k$ is equal to zero.

$$\boldsymbol{s}_k + \Delta\boldsymbol{s}_k = f_k\left(\boldsymbol{s}_{k-1} + \Delta\boldsymbol{s}_{k-1}, \boldsymbol{u}_{k-1} + \Delta\boldsymbol{u'}_{k-1}\right). \tag{9}$$

According to (5) and (6), (9) can be modified to

$$\boldsymbol{s}_k + \Delta\boldsymbol{s}_k = f_k\left(\boldsymbol{s}_{k-1}, \boldsymbol{u}_{k-1}\right) + \boldsymbol{A}_{k-1}\Delta\boldsymbol{s}_{k-1} + \boldsymbol{B}_{k-1}\Delta\boldsymbol{u'}_{k-1}, \tag{10}$$

where $\boldsymbol{A}_{k-1} = \frac{\partial f_k(\boldsymbol{s}_{k-1}, \boldsymbol{u}_{k-1})}{\partial \boldsymbol{s}_k}$, $\boldsymbol{B}_{k-1} = \frac{\partial f_k(\boldsymbol{s}_{k-1}, \boldsymbol{u}_{k-1})}{\partial \boldsymbol{u}_k}$.

Due to $\boldsymbol{s}_k = f_k\left(\boldsymbol{s}_{k-1}, \boldsymbol{u}_{k-1}\right)$, we have

$$\Delta\boldsymbol{s}_k = \boldsymbol{A}_{k-1}\Delta\boldsymbol{s}_{k-1} + \boldsymbol{B}_{k-1}\Delta\boldsymbol{u'}_{k-1}. \tag{11}$$

Defining the infinite regulator problem as

$$\boldsymbol{\zeta}_{\min} = \frac{1}{2}\Sigma_{k=0}^{\infty}\left(\Delta\boldsymbol{s}_k^T\boldsymbol{H}\Delta\boldsymbol{s}_k + \Delta\boldsymbol{u'}_{k-1}^T\boldsymbol{N}\Delta\boldsymbol{u'}_{k-1}\right), \tag{12}$$

where $\boldsymbol{H}$ is positive semi-definite matrix and $\boldsymbol{N}$ denotes positive definite matrix.

Assumption 1: The matric $\boldsymbol{A}_k = \left(\frac{\partial f_k^T}{\partial \boldsymbol{s}_k}\right)^T$, $\boldsymbol{B}_k = \left(\frac{\partial f_k^T}{\partial \boldsymbol{u}_k}\right)^T$, $\boldsymbol{C}_{k+1} = \left(\frac{\partial h_{k+1}^T}{\partial \boldsymbol{s}_{k+1}}\right)^T$ are bounded in $\boldsymbol{s}_k$ for all $\|\Delta\boldsymbol{s}_k\| \leq \varepsilon$, where ε is a positive scalar.

Assumption 2: The system is completely observable for the pair $(\boldsymbol{A}_k, \boldsymbol{B}_k)$. The system is completely controllable for the pair $(\boldsymbol{A}_k, \boldsymbol{C}_{k+1})$.

Under the assumption 1 and 2, the minimization of (12) subject to (11), getting the linear-quadratic optimum control

$$\Delta\boldsymbol{u'}_{k-1} = -\boldsymbol{K}_{k-1}\Delta\boldsymbol{s}_{k-1}, \tag{13}$$

where

$$\boldsymbol{K}_{k-1} = \boldsymbol{N}^{-1}\boldsymbol{B}_{k-1}^T\left(\boldsymbol{\pi}_{k-1}^{-1} + \boldsymbol{B}_{k-1}\boldsymbol{N}^{-1}\boldsymbol{B}_{k-1}^T\right)^{-1}\boldsymbol{A}_{k-1}, \tag{14}$$

and $\boldsymbol{\pi}_{k-1}$ is the solution of the Riccati matrix differential equation as follows

$$\boldsymbol{\pi}_{k-1} = \boldsymbol{H} + \boldsymbol{A}_{k-1}^T\left(\boldsymbol{\pi}_{k-1}^{-1} + \boldsymbol{B}_{k-1}\boldsymbol{N}^{-1}\boldsymbol{B}_{k-1}^T\right)^{-1}\boldsymbol{A}_{k-1}. \tag{15}$$

Substituting (13) into (10) produce

$$\boldsymbol{s}_{k+1} = f_k\left(\boldsymbol{s}_k, \boldsymbol{u}_{k-1}\right) - \boldsymbol{B}_{k-1}\boldsymbol{K}_{k-1}\Delta\boldsymbol{s}_{k-1}. \tag{16}$$

2) CORRECTIVE CONTROL

If the imposed constraint (2) is not satisfied, defining the static optimization problem as follows:

$$\begin{aligned}\boldsymbol{\zeta}_{\min} = &\frac{1}{2}\left(\tilde{\boldsymbol{s}}_{k+1} - \boldsymbol{s}_{k+1}\right)^T\boldsymbol{W}\left(\tilde{\boldsymbol{s}}_{k+1} - \boldsymbol{s}_{k+1}\right)\\ &+ \frac{1}{2}\Delta\boldsymbol{u''}_k^T\boldsymbol{M}\Delta\boldsymbol{u''}_k,\\ s.t.\ &\bar{\boldsymbol{P}}\left(\boldsymbol{s}_{k+1}\right) = \bar{\boldsymbol{p}}_{k+1},\end{aligned} \tag{17}$$

where $\boldsymbol{W}$ and $\boldsymbol{M}$ are positive definite matrices, $\tilde{\boldsymbol{s}}_{k+1}$ denotes the desired state vector with respect to $\Delta\boldsymbol{u''}_k$, $\bar{\boldsymbol{P}}\left(\boldsymbol{s}_{k+1}\right)$ represents the subset violated constraints, and $\bar{\boldsymbol{p}}_{k+1}$ indicates the violated time function.

Let the state vector $\tilde{\boldsymbol{s}}_{k+1} = \boldsymbol{s}_{k+1} + \Delta\boldsymbol{s}_{k+1}$, and there is $\tilde{\boldsymbol{s}}_{k+1} = f_k\left(\boldsymbol{s}_k, \boldsymbol{u}_k\right) + \boldsymbol{B}_{k-1}\Delta\boldsymbol{u''}_k$, it becomes

$$\Delta\boldsymbol{s}_{k+1} = \boldsymbol{B}_{k-1}\Delta\boldsymbol{u''}_k. \tag{18}$$

The constraints function can be expressed as follows:

$$\bar{\boldsymbol{P}}\left(\boldsymbol{s}_{k+1} + \Delta\boldsymbol{s}_{k+1}\right) = \bar{\boldsymbol{P}}\left(\boldsymbol{s}_{k+1}\right) + \bar{\boldsymbol{D}}_{k+1}\Delta\boldsymbol{s}_{k+1} = \bar{\boldsymbol{p}}_{k+1}, \tag{19}$$

where $\bar{\boldsymbol{D}}_{k+1} = \frac{\partial f_k(\boldsymbol{s}_{k-1}, \boldsymbol{u}_{k-1})}{\partial \boldsymbol{s}_k}$.

The Lagrangian of the optimization problem (17) can be constructed as

$$\begin{aligned}\min \boldsymbol{L} = &\frac{1}{2}\Delta\boldsymbol{u''}_k^T\left(\boldsymbol{B}_{k-1}^T\boldsymbol{W}\boldsymbol{B}_{k-1} + \boldsymbol{M}\right)\Delta\boldsymbol{u''}_k\\ &+ \boldsymbol{\lambda}^T\left(\bar{\boldsymbol{P}}\left(\boldsymbol{s}_{k+1}\right) + \bar{\boldsymbol{D}}_{k+1}\boldsymbol{B}_{k-1}\Delta\boldsymbol{u''}_k - \bar{\boldsymbol{p}}_{k+1}\right).\end{aligned} \tag{20}$$

Let $\frac{\partial \boldsymbol{L}}{\partial \Delta\boldsymbol{u''}_k} = 0$, we get

$$\Delta\boldsymbol{u''}_k = -\boldsymbol{\Psi}\boldsymbol{B}_{k-1}^T\bar{\boldsymbol{D}}_{k+1}^T\boldsymbol{\lambda}, \tag{21}$$

where $\boldsymbol{\Psi} = \left(\boldsymbol{B}_{k-1}^T\boldsymbol{W}\boldsymbol{B}_{k-1} + \boldsymbol{M}\right)^{-1}$. Let $\frac{\partial \boldsymbol{L}}{\partial \boldsymbol{\lambda}} = 0$, it follows that

$$\bar{\boldsymbol{P}}\left(\boldsymbol{s}_{k+1}\right) + \bar{\boldsymbol{D}}_{k+1}\boldsymbol{B}_{k-1}\Delta\boldsymbol{u''}_k - \bar{\boldsymbol{p}}_{k+1} = 0. \tag{22}$$

Combing (21) and (22), it becomes

$$\boldsymbol{\lambda} = -\left(\bar{\boldsymbol{D}}_{k+1}\boldsymbol{B}_{k-1}\boldsymbol{\Psi}\boldsymbol{B}_{k-1}^T\bar{\boldsymbol{D}}_{k+1}^T\right)^{-1}\left(\bar{\boldsymbol{p}}_{k+1} - \bar{\boldsymbol{P}}\left(\boldsymbol{s}_{k+1}\right)\right). \tag{23}$$

The state vector satisfies (17) is given by

$$\boldsymbol{s}_{k+1} = f_k\left(\boldsymbol{s}_k, \boldsymbol{u}_k\right) - \boldsymbol{B}_{k-1}\boldsymbol{\Psi}\boldsymbol{B}_{k-1}^T\bar{\boldsymbol{D}}_{k+1}^T\boldsymbol{\lambda}, \tag{24}$$

D. STABILITY ANALYSIS OF THE MULTI-ROBOT SYSTEM

In this section, the stability of the multi-robot system is investigated. The subscript "eq" denotes the equilibrium point.

Assumption 3: The equilibrium points $\boldsymbol{s}_{eq}$ is controllable and observable for the multi-robot system.

From the assumption 3 to have $\lim_{k\to\infty}\hat{\boldsymbol{s}}_{k|k} = \boldsymbol{s}_{eq}$. Let $\boldsymbol{A'}_k = \boldsymbol{A}_c + \Delta\boldsymbol{A'}_k$, $\hat{\boldsymbol{K}}_k = \boldsymbol{K}_{eq} + \Delta\hat{\boldsymbol{K}}_k$, $\boldsymbol{u}_k = \boldsymbol{u}_{eq} + \Delta\boldsymbol{u}_k$, where $\boldsymbol{A}_c$ is the closed loop matrix at the equilibrium $\boldsymbol{s}_{eq}$, and $\boldsymbol{u}_{eq}$ shows the steady state value of $\boldsymbol{u}_k$, with $\boldsymbol{u}_{-1} = \boldsymbol{0}$.

Combing (8) and (13), the closed loop control signal u_k can be reduced to

$$\begin{aligned}\boldsymbol{u}_k &= \boldsymbol{u'}_{k-1} + \Delta\boldsymbol{u'}_{k-1} + \boldsymbol{u''}_k + \Delta\boldsymbol{u''}_k \\ &= -\Sigma_{i=j}^{k}\left(\boldsymbol{K}_{eq} + \Delta\hat{\boldsymbol{K}}_{i-1}\right)\Delta\hat{\boldsymbol{s}}_{i-1|i-1} + \Sigma_{i=l}^{k}\Delta\boldsymbol{u''}_i \\ &= -\boldsymbol{K}_{eq}\left(\hat{\boldsymbol{s}}_{k|k} - \hat{\boldsymbol{s}}_{j-1|j-1}\right) - \Sigma_{i=j}^{k}\Delta\hat{\boldsymbol{K}}_{i-1}\Delta\hat{\boldsymbol{s}}_{i-1|i-1} + \boldsymbol{\wp}_k\hat{\boldsymbol{s}}_{k|k} \\ &= -\left(\boldsymbol{K}_{eq} + \boldsymbol{G}_k - \boldsymbol{\wp}_k\right)\hat{\boldsymbol{s}}_{k|k} \\ &= -\bar{\boldsymbol{K}}_k\hat{\boldsymbol{s}}_{k|k}, \end{aligned} \tag{25}$$

where j, l are the starting sample point at the gain and the corrective control action, respectively. $\boldsymbol{G}_k$ and $\boldsymbol{\wp}_k$ are gain matrix with adjustable elements.

Defining the error between the state $\boldsymbol{s}_k$ and the balance points $\boldsymbol{s}_{eq}$:

$$\delta\boldsymbol{s}_k = \boldsymbol{s}_k - \boldsymbol{s}_{eq}. \tag{26}$$

Thus, one obtains

$$\delta\hat{\boldsymbol{s}}_{k|k} = \hat{\boldsymbol{s}}_{k|k} - \boldsymbol{s}_{eq} = \delta\boldsymbol{s}_k - \boldsymbol{e}_{s_{k|k}}. \tag{27}$$

Let $\Delta\bar{\boldsymbol{K}}_k = \bar{\boldsymbol{K}}_k - \bar{\boldsymbol{K}}_{eq}$. Defining the deviation $\delta\boldsymbol{u}_k$:

$$\delta\boldsymbol{u}_k = \boldsymbol{u}_k - \boldsymbol{u}_{eq}. \tag{28}$$

Substituting (25) into (28) produce

$$\delta\boldsymbol{u}_k = -\bar{\boldsymbol{K}}_{eq}\delta\hat{\boldsymbol{s}}_{k|k} - \Delta\bar{\boldsymbol{K}}_k\hat{\boldsymbol{s}}_{k|k}. \tag{29}$$

The state vector $\boldsymbol{s}_{k+1}$ can be related as

$$\boldsymbol{s}_{k+1} = f\left(\boldsymbol{s}_{eq}, \boldsymbol{u}_{eq}\right) + \boldsymbol{A}_{eq}\delta\boldsymbol{s}_k + \boldsymbol{B}_{eq}\delta\boldsymbol{u}_k + \hat{\boldsymbol{\vartheta}}_k, \tag{30}$$

where $\hat{\boldsymbol{\vartheta}}_k$ represents the higher order terms in the Tailor series expansion. Let $\boldsymbol{s}_{eq} = f\left(\boldsymbol{s}_{eq}, \boldsymbol{u}_{eq}\right)$, $\delta\boldsymbol{s}_{k+1}$ can be expressed by

$$\begin{aligned}\delta\boldsymbol{s}_{k+1} &= \boldsymbol{s}_{k+1} - \boldsymbol{s}_{eq} \\ &= \boldsymbol{A}_{eq}\delta\boldsymbol{s}_k + \boldsymbol{B}_{eq}\delta\boldsymbol{u}_k + \hat{\boldsymbol{\vartheta}}_k \\ &= \left(\boldsymbol{A}_{eq} - \boldsymbol{B}_{eq}\bar{\boldsymbol{K}}_{eq}\right)\delta\boldsymbol{s}_k + \boldsymbol{B}_{eq}\bar{\boldsymbol{K}}_{eq}\boldsymbol{e}_{s_{k|k}} \\ &\quad - \boldsymbol{B}_{eq}\Delta\bar{\boldsymbol{K}}_k\hat{\boldsymbol{s}}_{k|k} + \hat{\boldsymbol{\vartheta}}_k. \end{aligned} \tag{31}$$

Defining $\boldsymbol{e}_{s_{k|k}} = \boldsymbol{s}_k - \hat{\boldsymbol{s}}_{k|k}$, and combining (7), we get

$$\boldsymbol{e}_{s_{k+1|k+1}} = \boldsymbol{A'}_k\boldsymbol{e}_{s_{k|k}} \tag{32}$$

Combining (31) and (32) produce

$$\boldsymbol{V}_{k+1} = \boldsymbol{\varsigma}_{eq}\boldsymbol{V}_k + \boldsymbol{\chi}_k\boldsymbol{V}_k + \boldsymbol{\rho}_k, \tag{33}$$

where $\boldsymbol{\varsigma}_{eq} = \begin{bmatrix} \boldsymbol{A}_{eq} - \boldsymbol{B}_{eq}\bar{\boldsymbol{K}}_{eq} & \boldsymbol{B}_{eq}\bar{\boldsymbol{K}}_{eq} \\ 0 & \boldsymbol{A}_c \end{bmatrix}$, $\boldsymbol{V}_k^T = \begin{bmatrix} \delta\boldsymbol{s}_k^T & \boldsymbol{e}_{s_{k|k}}^T \end{bmatrix}$, $\boldsymbol{\rho}_k = -\boldsymbol{B}_{eq}\Delta\bar{\boldsymbol{K}}_k\hat{\boldsymbol{s}}_{k|k} + \hat{\boldsymbol{\vartheta}}_k$, and $\boldsymbol{\chi}_k = \begin{bmatrix} 0 & 0 \\ 0 & \Delta\boldsymbol{A'}_k \end{bmatrix}$.

The homogenous equation of (34) can be written as

$$\boldsymbol{V'}_{k+1} = \boldsymbol{\varsigma}_{eq}\boldsymbol{V}_k\ (k \geq 0). \tag{34}$$

Assumption 4: The matrix $\lim_{k\to\infty} \boldsymbol{E}\left(\boldsymbol{\varsigma}_{eq} + \boldsymbol{\chi}_k\right) = \boldsymbol{\varsigma}_{eq}$ is a constant matrix, the solution of (34) remains bounded as k goes to infinity.

Theorem 1: Under the Assumption 1-4, the proposed observer-controller (8) can make the solution of (33) remains bounded. The convergences of the estimation error $\boldsymbol{e}_{s_{k|k}}$ and the position deviation $\delta\boldsymbol{s}_k$ are guaranteed. The multi-robot system (2) is asymptotically stable.

Proof: From the assumption 4 to have that (34) is bounded, so there is c_1 for $k \geq 0$ to satisfy that

$$\left\|\boldsymbol{\varsigma}_{eq}^{k+1}\right\| \leq c_1, \tag{35}$$

The transformation of (34) is equal to

$$\boldsymbol{V'}_{k+1} = \boldsymbol{\varsigma}_{eq}^{k+1}\boldsymbol{V}_0. \tag{36}$$

The solution of (33) can be written as

$$\boldsymbol{V}_{k+1} = \boldsymbol{\varsigma}_{eq}^{k+1}\boldsymbol{V}_0 + \Sigma_{j=0}^{k}\boldsymbol{\varsigma}_{eq}^{k-j}\left(\boldsymbol{\chi}_j\boldsymbol{V}_j + \boldsymbol{\rho}_j\right). \tag{37}$$

Let $\left\|\boldsymbol{\chi}_k\boldsymbol{V}_k\right\| = \alpha_k\left\|\boldsymbol{V}_k\right\|$, $\rho_k = \beta_k\left\|\boldsymbol{V}_k\right\|$. Combing (35) and (37), one obtains

$$\left\|\boldsymbol{V}_{k+1}\right\| \leq c_1\left\|\boldsymbol{V}_0\right\| + \boldsymbol{\Sigma}_{j=0}^{k}c_1\left(\alpha_j + \beta_j\right)\left\|\boldsymbol{V}_j\right\|. \tag{38}$$

According to Bellman-Gronwall inequality, (38) becomes

$$\left\|\boldsymbol{V}_{k+1}\right\| \leq c_1\left\|\boldsymbol{V}_0\right\|\exp\boldsymbol{\Sigma}_{j=0}^{k}c_1\left(\alpha_j + \beta_j\right). \tag{39}$$

Let $\Sigma_{k=0}^{\infty}\left(\alpha_k + \beta_k\right) < c_2$, (39) can be reduced to

$$\left\|\boldsymbol{V}_{k+1}\right\| \leq c_1\left\|\boldsymbol{V}_0\right\|\exp\left(c_1c_2\right). \tag{40}$$

This shows that the non-homogenous equation (33) is bounded. Since the designed closed loop matrices are asymptotically stable, it follows that

$$\left\|\boldsymbol{\varsigma}_{eq}^{k+1}\right\| \leq \tau^k, \tag{41}$$

where $0 < \tau < 1$ and $k \geq K$. Similar to (35)-(40), (33) can be modified by

$$\left\|\boldsymbol{V}_{k+1}\right\| \leq \tau^k\left\|\boldsymbol{V}_0\right\|\exp\left(c_1c_2\right). \tag{42}$$

Since $\lim_{k\to\infty}\tau^k = 0$, we have

$$\lim_{k\to\infty}\left\|\boldsymbol{V}_{k+1}\right\| = 0. \tag{43}$$

Therefore, the estimation error $\boldsymbol{e}_{s_{k|k}}$ and the position deviations $\delta\boldsymbol{s}_k$ can converge to zero. The multi-robot system (2) is locally exponentially stable.

Remark 1: In the existing results, there are few literatures have considered the sudden change of the given trajectory. In this paper, the proposed observer-based controller (8) which contains gain control and corrective control can guarantee the stability of the formation for the multi-robot system during trajectory transformation.

III. OBSTACLE AVOIDANCE

In this section, the obstacle avoidance of the multi-robot system is considered. Assuming that the formation has been formed before encountering an obstacle. The distance between the leader and the followers are $l_1 = 1.5m$ and $l_2 = 1.7m$. The detection range can be divided into five parts according to the size of formation as shown in Fig. 2.

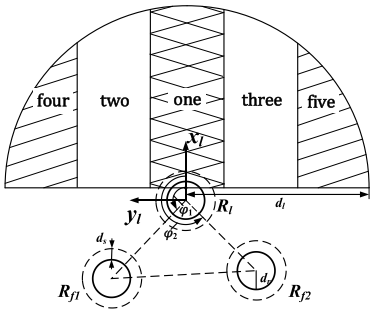

FIGURE 2. The detection range of the leader.

TABLE 1. The range of values for five parts.

Part	Range (y_l)
One	$[-(d_r+d_s)\ ,\ d_r+d_s]$
Two	$[d_r+d_s\ ,\ l_1 sin\varphi_1+d_r+d_s]$
Three	$[l_2 sin\varphi_2-(d_r+d_s)\ ,\ -(d_r+d_s)]$
Four	$[l_1 sin\varphi_1+d_r+d_s\ ,\ d_l]$
Five	$[-d_l\ ,\ l_2 sin\varphi_2-(d_r+d_s)]$

Where d_l is the maximum measured value of the transducer, d_r is the radius of robot, the range of values for each part can be described as Table. 1.

The safe threshold d_s is set to avoid collision, i.e. the minimum distance between robot and obstacle or between robots. The IOAA is as follows:

Step 1: Calculating the relative state $\boldsymbol{s}_{ob}^{l} = \left[\, x_{ob}^{l}\ y_{ob}^{l}\ \theta_{ob}^{l} \,\right]^T$ between the leader robot and the obstacles.

Step 2: Comparing y_{ob}^{l} with the range of values for five parts in Table. 1, and obtaining the regional distribution of obstacles.

Step 3: If obstacles appear in part one, the leader plans path to avoid collisions. Then stop. Else go to step 4.

Step 4: If obstacles are founded in part two and three, calculating $l_{ob} = \sqrt{\left(x_{ob1}^{l} - x_{ob2}^{l}\right)^2 + \left(y_{ob1}^{l} - y_{ob2}^{l}\right)^2}$ and $l_d = l_{ob} - (4d_r + 3d_s)$. Else go to step 8.

Step 5: If $l_d < 0$, the formation becomes a single column as Fig. 3(a). Then stop. Else go to step 6.

Step 6: If obstacles lie in part two, increasing the value of φ_1 until the condition $\varphi_1 \geq \pi - \sin^{-1}\left(\frac{y_1^l - d_r - d_s}{l_1}\right)$ is satisfied. Then stop. Else go to step 7.

Step 7: Decreasing φ_2 until $\varphi_2 \leq \pi - \sin^{-1}\left(\frac{y_2^l - d_r - d_s}{l_2}\right)$ is satisfied. Then stop.

Step 8: The formation and the path of the robot system remain unchanged. Then stop.

Remark 2: If the distance between the follower robots is too short in Fig. 3(b), it is necessary to add a constraint as follows in step 6 and 7 to avoid collision between robots:

$$\sqrt{\left(x_{f1} - x_{f2}\right)^2 + \left(y_{f1} - y_{f2}\right)^2} \geq d_s$$

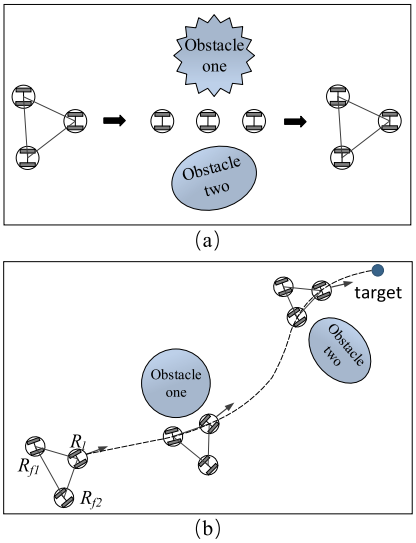

FIGURE 3. Cooperative obstacle avoidance: (a) shows the change of the formation, (b) shows the adjust of the formation.

Comparing with obstacle avoidance algorithm in the literatures [29]–[32], the main differences in this paper can be described as follows: 1) not only the obstacle avoidance between the robots and the obstacles is discussed, but also the collision avoidance between robots is considered. 2) The algorithm considers three different situations that could encounter in the process of obstacle avoidance and puts forward the optimal obstacle avoidance method correspondingly. In particular, the IOAA avoid obstacles by adjusting the angle between the leader and the followers, which can decrease the allocation of time compare to changing the formation and can short the distance compare to bypassing obstacles as a whole.

IV. SIMULATION

Simulations have been performed to demonstrate the validity of the proposed formation control method. Dividing the simulation into three parts.

The formation considered one leader robot and two follower robots. Let $\boldsymbol{s}_l(0) = \left[\, 2\ 2\ \pi/2 \,\right]^T$, $\boldsymbol{s}_{f1}(0) = \left[\, 1\ 2.2\ 2\pi/3 \,\right]^T$, $\boldsymbol{s}_{f2}(0) = \left[\, 2.3\ 1\ \pi/3 \,\right]^T$, the estimators are assumed to be $\hat{\boldsymbol{s}}_{f1}(0) = \left[\, 1.09\ 2.14\ 2\pi/3 \,\right]^T$, $\hat{\boldsymbol{s}}_{f2}(0) = \left[\, 2.24\ 1.08\ \pi/3 \,\right]^T$. The weighting matrices of the cost function (14) are $\boldsymbol{H} = 10\boldsymbol{I}_3$, $\boldsymbol{N} = 10\boldsymbol{I}_2$, the cost function (20) are $\boldsymbol{W} = diag\left\{\, 1\ 1\ 1 \,\right\}$, $\boldsymbol{M} = diag\left\{\, 100\ 10 \,\right\}$. The sampling period is $T_c = 0.01s$.

In the first part, considering only the gain control. The following velocity are assigned to the leader robot:

$$p: \begin{cases} v_l(t) = 0.98m/s \\ \omega_l(t) = -\sin(1.1t). \end{cases}$$

Fig. 4 shows the trajectories of the multi-robot system. It is noticeable that the follower robot R_{f1} makes adjustment accordingly, because the initial direction is different from the leader robot. The desired formation is properly maintained in

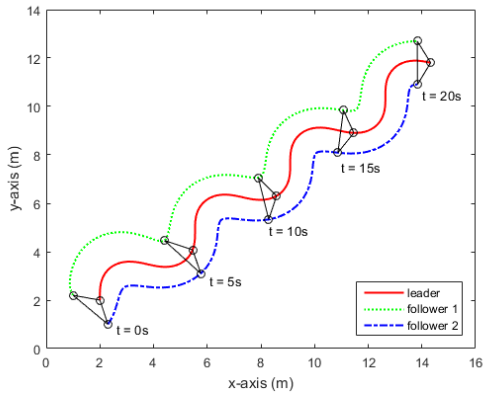

FIGURE 4. Trajectory of the robots.

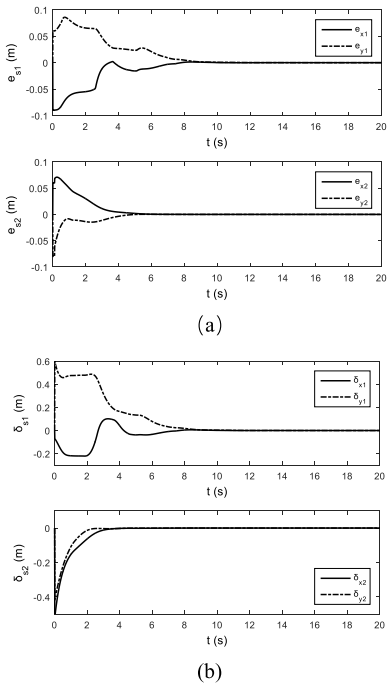

FIGURE 5. Simulation results: (a) shows the estimation errors, (b) shows the position deviations.

the subsequent movement. Fig. 5(a) illustrates the estimation errors between the actual state and the estimated state of the follower robots. Fig. 5(b) shows the position deviations between the actual state and the equilibrium state of the follower robots. It confirms the theoretical conclusion in Theorem 1 and indicates that the proposed algorithm enables the follower robots track the leader.

In the second part, considering both the gain control and the corrective control. In gain control part, the velocities of the leader robot are

$$p: \begin{cases} v_l(t) = 0.98m/s \\ \omega_l(t) = -0.9\sin(1.1t). \end{cases}$$

After adding corrective control, the velocities are

$$\bar{p}: \begin{cases} v_l(t) = 0.98m/s \\ \omega_l(t) = 0.9\sin(1.1t). \end{cases}$$

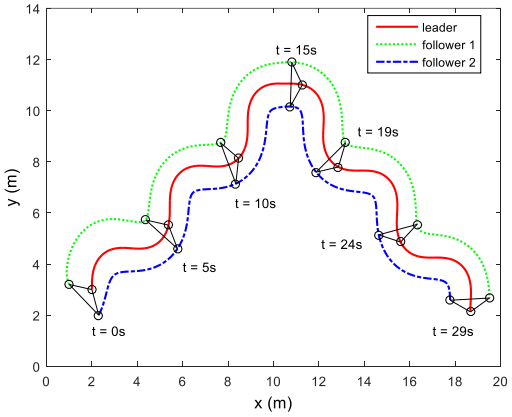

FIGURE 6. Trajectory of the robots.

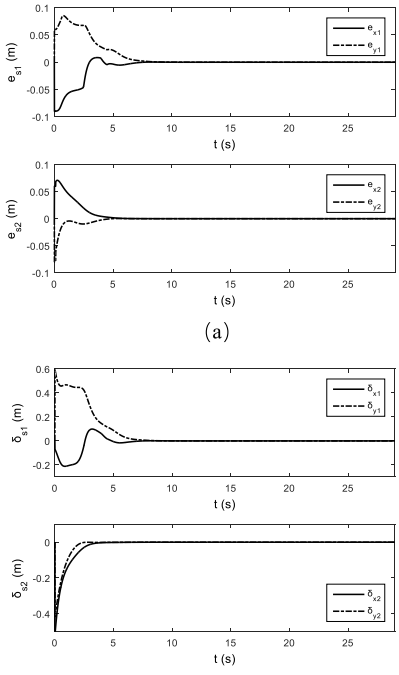

FIGURE 7. Simulation results: (a) shows the estimation errors with the trajectory transformation at $t = 14s$, (b) shows the position deviations with the trajectory transformation at $t = 14s$.

Fig. 6 shows the trajectories of the leader and the follower robots. Comparing to Fig 4, it is apparently that the trajectories changed at $t = 14s$ due to the imposed constraint (2) is not satisfied. The convergence of the estimation errors and position deviations was confirmed in Fig. 7.

In the third part, the obstacle avoidance is considered. Setting the position of the obstacles $x_{ob1} = \begin{bmatrix} 5.1 & 6.7 \end{bmatrix}^T$ and $x_{ob2} = \begin{bmatrix} 11.5 & 5.3 \end{bmatrix}^T$, The safe threshold $d_s = 0.6m$.

Fig. 8 demonstrates the trajectories of obstacle avoidance for multi-robot system. In the initial phase, three robots maintain triangle formation and the leader R_l can be traced by the follower R_f. The formation is changed according to the value of distance and angle between leader robot and follower robots, i.e., $(l_1, \varphi_1)^T$ and $(l_2, \varphi_2)^T$. Avoiding obstacles by adjusting the angle φ_1 and φ_2 of robots.

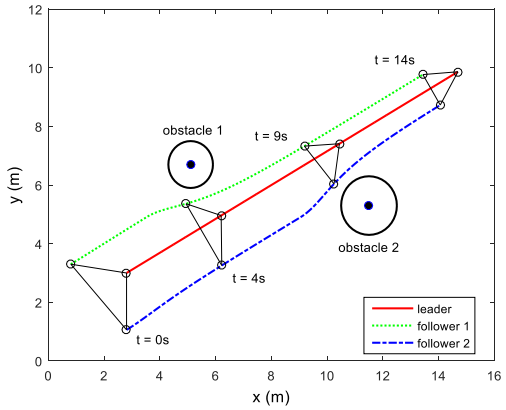

FIGURE 8. **Obstacle avoidance.**

V. CONCLUSION

This paper proposed an observer-based trajectory tracking strategy for the multi-robot. First, the leader robot followed the given trajectory and the followers tracked the leader according to the formation control law. An observer was devised to estimate the state of the leader robot. Then, gain control and corrective control were presented. The former completes the formation task and the latter implements the trajectory transformation. Moreover, the stability theorem was obtained to prove the convergence of the estimation errors and the position deviations. In addition, the IOAA for the multi-robot system was designed to reduce the time allocation of obstacle avoidance. The IOAA was implemented by adjusting the angle between the leader robot and the followers. Finally, simulation results were presented to verify the effectiveness of the proposed control scheme. Future research for multi-robot formation control include the study of the path planning based on fractional-order controller.

ACKNOWLEDGEMENT

The authors report no conflicts of interest in conducting the research.

REFERENCES

[1] H. Wang, P. X. Liu, S. Li, and D. Wang, "Adaptive neural output-feedback control for a class of nonlower triangular nonlinear systems with unmodeled dynamics," *IEEE Trans. Neural Netw. Learn. Syst.*, vol. 29, no. 8, pp. 3658–3668, Aug. 2018.

[2] X. Zhao, X. Wang, G. Zong, and H. Li, "Fuzzy-approximation-based adaptive output-feedback control for uncertain nonsmooth nonlinear systems," *IEEE Trans. Fuzzy Syst.*, vol. 26, no. 6, pp. 3847–3859, Dec. 2018.

[3] H. Wang, P. X. Liu, and B. Niu, "Robust fuzzy adaptive tracking control for nonaffine stochastic nonlinear switching systems," *IEEE Trans. Cybern.*, vol. 48, no. 8, pp. 2462–2471, Aug. 2018.

[4] X. Zhao, P. Shi, and X. Zheng, "Fuzzy adaptive control design and discretization for a class of nonlinear uncertain systems," *IEEE Trans. Cybern.*, vol. 46, no. 6, pp. 1476–1483, Jun. 2016.

[5] D. Wang, D. Liu, C. Mu, and Y. Zhang, "Neural network learning and robust stabilization of nonlinear systems with dynamic uncertainties," *IEEE Trans. Neural Netw. Learn. Syst.*, vol. 29, no. 4, pp. 1342–1351, Apr. 2018.

[6] G. Lee and D. Chwa, "Decentralized behavior-based formation control of multiple robots considering obstacle avoidance," *Intell. Service Robot.*, vol. 11, no. 1, pp. 127–138, 2018.

[7] F. Bayat, S. Najafinia, and M. Aliyari, "Mobile robots path planning: Electrostatic potential field approach," *Expert Syst. Appl.*, vol. 100, pp. 68–78, Jun. 2018.

[8] B. M. Ferreira, A. C. Matos, N. A. Cruz, and A. P. Moreira, "Coordination of marine robots under tracking errors and communication constraints," *IEEE J. Ocean. Eng.*, vol. 41, no. 1, pp. 27–39, Jan. 2016.

[9] Y. Yang, D. Yue, and C. Dou, "Output-based event-triggered schemes on leader-following consensus of a class of multi-agent systems with Lipschitz-type dynamics," *Inf. Sci.*, vol. 459, pp. 327–340, Aug. 2018.

[10] R. Sakthivel, R. Sakthivel, and B. Kaviarasan, "Leader-following exponential consensus of input saturated stochastic multi-agent systems with Markov jump parameters," *Neurocomputing.*, vol. 287, pp. 84–92, Apr. 2018.

[11] A. Denasi and S. Misra, "Independent and leader–follower control for two magnetic micro-agents," *IEEE Robot. Autom. Lett.*, vol. 3, no. 1, pp. 218–225, Jan. 2018.

[12] C. Unsalan and B. Sirmacek, "Road network detection using probabilistic and graph theoretical methods," *IEEE Trans. Geosci. Remote Sens.*, vol. 50, no. 11, pp. 4441–4453, Nov. 2012.

[13] E. Montijano, E. Cristofalo, D. Zhou, M. Schwager, and C. Sagüés, "Vision-based distributed formation control without an external positioning system," *IEEE Trans. Robot.*, vol. 32, no. 2, pp. 339–351, Apr. 2016.

[14] K.-C. Cao, B. Jiang, and D. Yue, "Rendezvous of multiple nonholonomic unicycles-based on backstepping," *Int. J. Control*, vol. 91, no. 6, pp. 1271–1283, 2018.

[15] R. Li, L. Zhang, L. Han, and J. Wang, "Multiple vehicle formation control based on robust adaptive control algorithm," *IEEE Intell. Transp. Syst. Mag.*, vol. 9, no. 2, pp. 41–51, Apr. 2017.

[16] X. Xing, Z. X. Peng, G. G. Wen, and A. Rahmani, "Distributed fixed-time formation tracking of multi-robot systems with nonholonomic constraints," *Neurocomputing*, vol. 313, pp. 167–174, Nov. 2018.

[17] A. Lopez-Gonzalez, E. D. Ferreira, E. G. Hernandez-Martinez, J.-J. Flores-Godoy, G. Fernandez-Anaya, and P. Paniagua-Contro, "Multi-robot formation control using distance and orientation," *Adv. Robot.*, vol. 30, no. 14, pp. 901–913, 2016.

[18] M. Hassan, E. Aljuwaiser, and R. Badr, "A new on-line observer-based controller for leader-follower formation of multiple nonholonomic mobile robots," *J. Franklin Inst.*, vol. 355, pp. 2436–2472, Mar. 2018.

[19] C. Yang, L. Y. Zhang, C. Y. Li, and M. Z. Q. Chen, "Observer-based consensus tracking of nonlinear agents in hybrid varying directed topology," *IEEE J. Mag.*, vol. 47, no. 8, pp. 2212–2222, Aug. 2017.

[20] A. Ahmad, G. Lawless, and P. Lima, "An online scalable approach to unified multirobot cooperative localization and object tracking," *IEEE Trans. Robot.*, vol. 33, no. 5, pp. 1184–1199, Oct. 2017.

[21] T. Sun, F. Liu, H. Pei, and Y. He, "Brief paper-observer-based adaptive leader-following formation control for non-holonomic mobile robots," *IET Control Theory Appl.*, vol. 6, no. 18, pp. 2835–2841, 2012.

[22] Z. X. Zhong, Y. Z. Zhu, and C. K. Ahn, "Reachable set estimation for Takagi-Sugeno fuzzy systems against unknown output delays with application to tracking control of AUVs," *ISA Trans.*, vol. 78, pp. 31–38, Jul. 2018.

[23] K. Shojaei, "Neural adaptive PID formation control of car-like mobile robots without velocity measurements," *Adv. Robot.*, vol. 31, no. 18, pp. 947–964, 2017.

[24] J. Wang, P. Zhang, and W. Ni, "Observer-based event-triggered control for consensus of general linear MASs," *IET Control Theory Appl.*, vol. 11, no. 18, pp. 3305–3312, 2017.

[25] G. H. Wen, T. W. Huang, W. W. Yu, Y. Q. Xia, and Z.-W. Liu, "Cooperative tracking of networked agents with a high-dimensional leader: Qualitative analysis and performance evaluation," *IEEE Trans Cybern.*, vol. 48, no. 7, pp. 2060–2073, Jul. 2018.

[26] R. R. Nair and L. Behera, "Robust adaptive gain higher order sliding mode observer based control-constrained nonlinear model predictive control for spacecraft formation flying," *IEEE/CAA J. Autom. Sinica*, vol. 5, no. 1, pp. 367–381, Jan. 2018.

[27] L. Sabattini, C. Secchi, and C. Fantuzzi, "Coordinated dynamic behaviors for multirobot systems with collision avoidance," *IEEE Trans. Cybern.*, vol. 47, no. 12, pp. 4062–4073, Dec. 2017.

[28] J. Kim, "Cooperative exploration and networking while preserving collision avoidance," *IEEE Trans. Cybern.*, vol. 47, no. 12, pp. 4038–4048, Dec. 2017.

[29] D. Panagou and V. Kumar, "Cooperative visibility maintenance for leader–follower formations in obstacle environments," *IEEE Trans. Robot.*, vol. 30, no. 4, pp. 831–844, Aug. 2014.

[30] S.-M. Lee and H. Myung, "Receding horizon particle swarm optimisation-based formation control with collision avoidance for non-holonomic mobile robots," *IET Control Theory Appl.*, vol. 9, no. 14, pp. 2075–2083, 2015.
[31] G. Wen, C. L. P. Chen, and Y.-J. Liu, "Formation control with obstacle avoidance for a class of stochastic multi-agent systems," *IEEE Trans. Ind. Electron.*, vol. 65, no. 7, pp. 5847–5855, Jul. 2018.
[32] T. Mylvaganam and M. Sassano, "Autonomous collision avoidance for wheeled mobile robots using a differential game approach," *Eur. J. Control*, vol. 40, pp. 53–61, Mar. 2018.

XIRU WU received the Ph.D. degree in control science and engineering from Hunan University, Hunan, China. He is currently an Associate Professor with the Guilin University of Electronic Technology, Guangxi. His current research interests include robot control, neural networks, and deep learning.

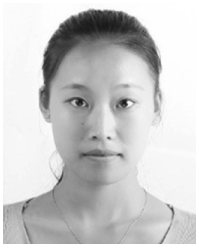

SHANSHAN WANG is currently pursuing the master's degree with the College of Electronic Engineering and Automation, Guilin University of Electronic Technology, Guangxi, China. Her research interest includes formation control of multi-robot.

MENGYUAN XING is currently pursuing the master's degree with the College of Electronic Engineering and Automation, Guilin University of Electronic Technology, Guangxi, China. Her research interest includes robot control.